

Multilevel and hierarchical Bayesian modeling of cosmic populations*

Thomas J. Loredo¹ and Martin A. Hendry²

¹*Cornell Center for Astrophysics and Planetary Science, Cornell University*

²*School of Physics & Astronomy, University of Glasgow*

Abstract: Demographic studies of cosmic populations must contend with measurement errors and selection effects. We survey some of the key ideas astronomers have developed to deal with these complications, in the context of galaxy surveys and the literature on corrections for Malmquist and Eddington bias. From the perspective of modern statistics, such corrections arise naturally in the context of multilevel models, particularly in Bayesian treatments of such models: hierarchical Bayesian models. We survey some key lessons from hierarchical Bayesian modeling, including shrinkage estimation, which is closely related to traditional corrections devised by astronomers. We describe a framework for hierarchical Bayesian modeling of cosmic populations, tailored to features of astronomical surveys that are not typical of surveys in other disciplines. This thinned latent marked point process framework accounts for the tie between selection (detection) and measurement in astronomical surveys, treating selection and measurement error effects in a self-consistent manner.

1 Introduction

Surveying the Universe is the ultimate remote sensing problem. Inferring the intrinsic properties of the galaxy population, via analysis of survey-generated catalogs, is a major challenge for twenty-first century cosmology, but this challenge must be met without any prospect of measuring these properties *in situ*. Thus, for example, our

*The main text of this paper is an update of “Bayesian multilevel modelling of cosmological populations,” which appeared in *Bayesian Methods in Cosmology* (ed. by M. P. Hobson, A. H. Jaffe, A. R. Liddle, P. Mukherjee, D. Parkinson), Cambridge University Press, pp. 245–264 (2010) (DOI). The Appendix is drawn from a monograph in preparation; the authors would be grateful for comments on the new material.

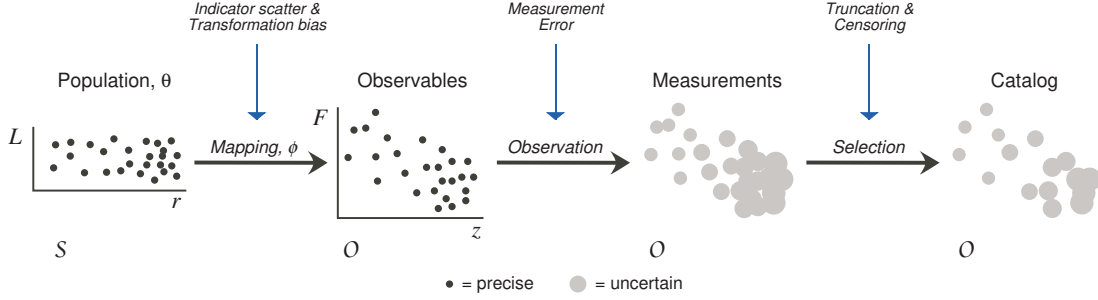


Figure 1: Schematic depiction of the survey process. A population with a distribution of source or object properties, \mathcal{S} (e.g., luminosity and distance), implies, via a mapping ϕ , a distribution of observables, \mathcal{O} (e.g., flux and redshift). Observation introduces measurement error; selection criteria thin, truncate, or censor the cataloged population.

knowledge of the intrinsic luminosity and spatial distribution of galaxies is filtered by imperfect distance information and by observational selection effects—issues which have come to be known generically in the literature as “Malmquist bias.”¹ Figure 1 shows schematically how such effects may distort our inferences about the underlying population since in general these must be derived from a noisy, sparse and truncated sample of galaxies.

There is a long (and mostly honourable!) tradition in the astronomical literature of attempts to cast such remote surveying problems within a rigorous statistical framework. Indeed, it is interesting to note that seminal examples from the early twentieth century—e.g., Eddington (1913, 1940); Malmquist (1920, 1922)—display, at least with hindsight, hints of a Bayesian formulation long before the recent renaissance of Bayesian methods in astronomy. Space does not permit us to review in detail that early literature, nor many of the more recent papers which evolved from it. A more thorough discussion of the early literature on statistical analysis of survey data can be found in, e.g., Hendry and Simmons (1995), Strauss and Willick (1995), Teerikorpi (1997), and Loredó (2007).

The analysis of survey catalogs can have a number of scientific goals. For example, the objective may be to compare the underlying galaxy luminosity distribution with the predictions of different galaxy formation models. In this case the galaxy distances (which we must infer as an intermediate step towards estimating their luminosities) are, in statistical parlance, nuisance parameters. On the other hand, the goal may

¹Although “Malmquist” is the most prevalent appellation, the literature also uses other terms—including “Eddington-Malmquist” and “Lutz-Kelker”—to denote biases arising in astronomical surveys from distance indicator scatter and observational selection. There is also an unfortunate history in the cosmology literature of the same term being used to mean substantially different things by different authors. For a more detailed account of the meaning, use, and abuse of bias terminology see, e.g., Hendry and Simmons (1995), Strauss and Willick (1995) and Teerikorpi (1997).

be to infer the distances of the surveyed galaxies, in order to test models of galaxy clustering and/or constrain parameters of the underlying cosmology. In this case it is the inferred galaxy luminosities (or other properties) which may be thought of as nuisance parameters.

In the literature of the past 25 years, the second case—that of inferring galaxy distances—has proven to be fertile territory for the development and application of Bayesian methods. This is particularly true with regard to (largely) redshift-independent distance indicators, i.e., indicators whose behaviour is independent of the underlying cosmological model (and which may thus be straightforwardly used to constrain parameters of that model). A likely reason for this is that redshift-independent distance indicators suffer from large intrinsic scatter, with distance uncertainties to individual galaxies typically in the range 5% to 30%. A consequence is that care must be taken when incorporating prior distance information, since in this setting final inferences can be significantly influenced by the prior, a point we discuss further in Section 2.

Another hallmark of the literature on extracting information from galaxy surveys has been the recognition by some authors (e.g., Hendry and Simmons 1995; Loredó 2007) that the task of identifying “optimal” (e.g., in the sense of unbiased and/or minimum mean square error) estimators of galaxy distance and luminosity will generally not have a unique solution, but will depend of the context in which the inferred galaxy distances or luminosities are to be used.

In Section (3) we discuss how multilevel models, and particularly hierarchical Bayesian models provide a natural, powerful framework in which to formulate and implement optimal analyses of surveys, incorporating prior information and carefully accounting for selection effects and source or object uncertainties. To motivate this approach, and to establish context, in Section (2) we survey key Bayesian elements of recent methodology for analysis of survey data, focusing on use of redshift-independent distance indicators, and highlighting examples which have previously hinted at a multilevel approach.

2 Galaxy distance indicators

While astrometric space missions (e.g. *Gaia*) offer some prospect of applying trigonometric methods over nearby cosmological scales, in large part the measurement of galaxy distances relies on more astrophysical, and therefore less precise, methods. Perhaps most obvious among these methods is the cosmological redshift. To derive a distance measure from it requires the use of a cosmological model. But if one’s goal is to use galaxy distance estimates to probe the parameters of the cosmological model, the safest path is to identify galaxy distance indicators whose properties are largely independent of redshift.

Almost all redshift-independent distance indicators are really *luminosity* or *size* indicators: one uses the indicator to estimate the intrinsic luminosity or size of a galaxy (or some object therein); combined with a measurement of its apparent brightness or apparent size, one may estimate distance via the inverse-square law or the angle-distance relation (or their cosmological generalisations). For simplicity we consider here only the case of luminosity indicators, although very similar statistical considerations apply to other types of indicator. We can estimate the luminosity either by assuming a constant, fiducial value (the so-called ‘standard candle’ assumption) or, better, by exploiting correlations between luminosity and some other intrinsic, but directly measurable, physical characteristic(s) of the source. (The latter approach is often referred to as a ‘standardisable candle.’) Examples of these correlations include: the Tully-Fisher relation for spiral galaxies; the period-luminosity relation for Cepheid variables and the luminosity–light curve shape relation for type Ia supernovae. The correlations may be motivated by theory, but they must be calibrated empirically, e.g., using nearby galaxies at known distances (and hence of known luminosity). Their scatter, reflecting the intrinsic spread in luminosity of the objects, renders distance indicators susceptible to observational selection biases since one cannot observe arbitrarily faint objects to arbitrary distances.

Since the late 1980s several authors have investigated the statistical properties of redshift-independent galaxy distance indicators, with the goal of placing their use in cosmology on a more rigorous statistical footing. A significant step forward in this regard came in the early 1990s with the work of Jeffrey Willick (1994), which brought much needed clarity to the discussion by explicitly making a distinction between the tasks of *calibrating* a distance indicator and applying it to a galaxy survey to *estimate* distances. We now briefly summarise the formalism presented in Willick (1994) and adopted in subsequent papers.

2.1 The calibration problem

Our starting point is the joint probability distribution for a single galaxy’s distance, r , apparent magnitude, m , and some third observable correlated with luminosity which, following Willick, we denote by η and refer to as the ‘line width’ parameter. As a concrete example, consider the Tully-Fisher relation, for which we expect the intrinsic relation between absolute magnitude and η to be linear, i.e. $M = a\eta + b$, where the coefficients a and b must be calibrated empirically. As noted earlier, an analysis may have various goals: a and b may simply be nuisance parameters, necessary to estimate galaxy distances; alternatively, they may be important target parameters in their own right.

Thus, for the joint probability density function (PDF) describing the properties

of galaxies within a particular survey catalog, we have

$$p(r, m, \eta) \propto r^2 n(r) S(m, \eta) \psi(m|\eta) \phi(\eta), \quad (1)$$

where $n(r)$ and $\phi(\eta)$ denote the marginal distributions of distance and line width respectively for the galaxy population (we will assume r and η are independent), $\psi(m|\eta)$ denotes the conditional distribution of apparent magnitude at a given line width (which depends on unknown parameters, e.g., a and b), and $S(m, \eta)$ denotes the observational selection effects (a detection probability, assumed here, for simplicity, not to depend on distance or direction).

Consider first the calibration of the distance indicator, which might reasonably be carried out, e.g., using a galaxy cluster, so the set of calibrators are effectively all at the same distance.² In this case it is natural to work with the conditional distribution of m at given η and r (i.e., the result from using equation (1) as a prior in Bayes' theorem, with a "likelihood" corresponding to precise measurement of η and r). Then the indicator coefficients a and b can be interpreted as the slope and zero-point of a linear regression of absolute magnitude on η —this case is known as the 'direct' indicator relation. Thus

$$P(m|\eta, r) = \frac{S(m, \eta) \psi(m|\eta)}{\int_{-\infty}^{\infty} S(m, \eta) \psi(m|\eta) dm}. \quad (2)$$

Notice that, as expected, the marginal distributions of distance and line width drop out. The presence of the observational selection effects will bias the determination of the indicator coefficients a and b obtained via simple linear regression; however, Willick (1994) proposed an iterative scheme to overcome this problem and showed that it works well for realistic mock galaxy data.

A popular variant on the above approach is to use the so-called 'inverse' relation, i.e. (in Willick's notation) $\eta^0(M) = a'M + b'$, where the inverse coefficients a' and b' again must be determined empirically (and again may be regarded either as nuisance parameters or target parameters). This relation is most directly expressed by the conditional distribution of η at a given r and m (corresponding to given M , since we are assuming all the calibrators lie at the same distance), namely

$$p(\eta|m, r) = \frac{S(m, \eta) \Psi(\eta|m)}{\int_{-\infty}^{\infty} S(m, \eta) \psi(\eta|m) d\eta}, \quad (3)$$

where Ψ denotes the conditional distribution of line width at given apparent magnitude (i.e., the reverse of the conditioning in $\psi(m|\eta)$). In this case explicit dependence

²Willick also considers the calibrators at a range of true distances; this case lends itself well to a Bayesian multilevel formulation, as we discuss in Section (3)

on the galaxy luminosity function (the distribution for M) drops out of our expression (because conditioning on (m, r) amounts to conditioning on M). Moreover, one can see that *if* the selection effects depend only on apparent magnitude and not on line width, then a straightforward linear regression of η on M *will* yield unbiased estimates of the indicator coefficients a' and b' . This appealing property of the inverse indicator relation had been recognised in principle much earlier by Schechter (1980) and was also placed on a rigorous statistical footing around the same time as Willick by Hendry and Simmons (1994). However, the successful calibration of a galaxy distance indicator is only the first part of the story.

2.2 The estimation problem

Suppose one has used the relations above to accurately and precisely calibrate a distance indicator (e.g., a and b are now precisely known). Now we seek to use the indicator in settings where there is no direct measurement of r ; we must infer r from measurements of m and η . We can calculate a predicted galaxy distance, d , in the obvious way by combining the observed apparent magnitude of the galaxy with its estimated absolute magnitude inferred (via our indicator relation) from its observed line width. Moreover, since $d = d(m, \eta)$, it is straightforward to compute the joint distribution, $p(r, d)$, of true and estimated galaxy distance, and further to determine the conditional distribution of r given d . For the direct indicator we obtain

$$p(r|d) = \frac{r^2 n(r) \exp\left(-\frac{[\ln r/d]^2}{2\Delta^2}\right)}{\int_0^\infty r^2 n(r) \exp\left(-\frac{[\ln r/d]^2}{2\Delta^2}\right) dr}, \quad (4)$$

where Δ is a constant describing the scatter in the direct indicator relation, i.e. the dispersion of the conditional distribution of absolute magnitude at given line width (here assumed Gaussian). For the inverse indicator, on the other hand, we obtain

$$p(r|d) = \frac{r^2 n(r) s(r) \exp\left(-\frac{[\ln r/d]^2}{2\Delta^2}\right)}{\int_0^\infty r^2 n(r) s(r) \exp\left(-\frac{[\ln r/d]^2}{2\Delta^2}\right) dr}, \quad (5)$$

where $s(r)$ is an integral over the galaxy luminosity function weighted by the selection effects, and expresses the probability that a galaxy at true distance r would be observable in the survey. This term is often referred to as the *selection function* for r .

The interpretation of equations ((4)) and ((5)) within the framework of Bayesian inference is clear. We can think of $p(r|d)$ as representing the posterior distribution of true distance r , given some observed data d (i.e. the estimated distance, from

our indicator). Moreover the *difference* between the two expressions can then be interpreted in terms of the adoption of different prior information for r : for the direct indicator the prior information is the true distance distribution $n(r)$, while for the inverse relation the prior is the product of $n(r)$ and the selection function.

The classical Malmquist bias is manifest when we take the conditional expectation of r given d , using equations ((4)) and ((5)). For both direct and inverse indicators we find that in general $E(r|d) \neq d$. However we can correct our ‘raw’ distance indicator d , defining d_{corr} which satisfies

$$E(r|d_{\text{corr}}) = d_{\text{corr}}, \quad (6)$$

with the correction term referred to as a “Malmquist correction.” Note, however, that the Malmquist correction depends explicitly on the true distance distribution $n(r)$, which in general will be unknown. Lynden-Bell et al. (1988) computed homogeneous Malmquist corrections, assuming that the underlying spatial distribution of galaxies is uniform, in which case

$$E(r|d) = d \exp\left(\frac{7}{2}\Delta^2\right) \simeq d \left(1 + \frac{7}{2}\Delta^2\right) \equiv d_{\text{corr}}. \quad (7)$$

We should not be surprised that the correction is always positive in this case; since we are assuming homogeneity we are saying that the distance indicator scatter is more likely to scatter galaxies *downwards* from greater true distances, simply because there are more galaxies at larger r due to the rapid growth of the volume element with r . Note, however, that for the inverse indicator the assumption of a uniform prior is not appropriate: even if $n(r)$ were constant, the selection function $s(r)$ clearly will not be.

The more realistic case is, of course, where the intrinsic distribution of distance is *not* uniform. In this case the adoption of a suitable prior for $n(r)$ leads to a so-called *inhomogeneous Malmquist correction*. For the direct indicator the source of the prior information could be, for example, the underlying density field of galaxies reconstructed from an external source, e.g., an all-sky redshift survey (c.f. Hudson 1994; Strauss and Willick 1995; Freudling et al. 1995; Ergogdu et al. 2006). The Malmquist corrections will only be valid in this case, however, provided that the external galaxy survey traces the same underlying population as the galaxies to which the distance indicator is being applied.

In an important paper, Landy and Szalay (1992) proposed an interesting alternative approach, whereby the marginal distribution of raw distances might provide a suitable estimate of the prior true distance distribution. Crucially, this method should *not* be applied using the direct indicator since the marginal distribution of raw distances provides a poor estimate of $n(r)$. On the other hand, it *does* provide a reasonable proxy for the distribution of true distances for ‘observable’ galaxies—i.e.

the product of $n(r)$ and $s(r)$. Thus, it is probably well suited to use with the inverse indicator.

The Landy and Szalay approach, although invoking implicit approximations, has several attractive features. It offers a method of defining inhomogeneous Malmquist corrections that adapts to spatial inhomogeneity, without requiring external assumptions or prior information about $n(r)$ from other galaxy surveys. Indeed it appears to be an approximation to a hierarchical Bayesian procedure, as we discuss further in Section 3.

2.3 Applications of galaxy distance indicators

Why might we regard Malmquist-corrected distance indicators, which satisfy equation ((6)), as optimal estimators in the first place? The answer lies largely in the uses to which they have been put. In the late 1980s redshift-independent distance indicators began to be used to measure galaxy *peculiar velocities*—the motions, over and above the Hubble expansion, induced by the net gravitational attraction of the matter distribution around them. Methods of analysing peculiar velocities generally involve first binning and grouping galaxies together based on their *estimated* distance. By requiring that on average the true distance of each galaxy be equal to its estimated distance, one aims to ensure that on average the correct radial peculiar velocity will be ascribed to each galaxy’s apparent position.

In the 1990s astronomers developed a number of sophisticated methods to compare observed and predicted galaxy peculiar velocities, the latter the result of reconstructing the density and peculiar velocity field from position and redshift data from an all-sky redshift survey. This reconstruction requires a model for *galaxy biasing*—i.e., a description of how the distribution of luminous galaxies and dark matter are related. By comparing observed and predicted peculiar velocities one can constrain parameters of the galaxy biasing model.

From a Bayesian perspective probably the most notable of these comparison methods was VELMOD (Willick and Strauss 1998). This assumed a simple linear relation between the galaxy and matter density fields and computed a posterior distribution for the linear bias parameter, marginalized over the nuisance parameters of the distance indicator relation. In its explicit modeling of the galaxy distance uncertainties, en route to estimating the linear bias parameter, VELMOD shares features with the hierarchical Bayesian approach which we now describe.

3 Multilevel, hierarchical Bayesian models

The issues motivating the astronomical developments just surveyed are hardly unique to astronomy. Statisticians have addressed similar issues in applications spanning

many disciplines. Although none of the resulting methods is an “exact fit” to an astronomical survey problem, the body of literature offers numerous insights that are inspiring significant advances in Bayesian methodology for astronomical surveys.

A recurring theme of much of the relevant literature is the use of *hierarchical Bayesian models* (HBMs). These are a subclass of *probabilistic graphical models*, and represent a Bayesian treatment of *multilevel models* (MLMs, terminology used in both Bayesian and frequentist literature). These terms cover a rich framework that underlies several important statistical innovations of the latter 20th century, including empirical Bayes methods, random effects and latent variable models, shrinkage estimation, and ridge regression. MLMs start with a *lower level* probability model for the data, given *latent parameters* specifying the properties of members of the surveyed population (e.g., objects or sources). This level typically describes noise and other aspects of the individual member measurement process. The *upper level* assigns a shared prior distribution to the lower-level parameters (e.g., a population-level distribution for object properties); this distribution may itself have unknown parameters, dubbed *hyperparameters*. The upper level leads to probabilistic dependence among the lower-level latent parameters that implements a pooling of information that can improve the accuracy of inferences; one says the estimates “borrow strength” from each other. Other levels may be added, e.g., to describe relationships between groups of objects.

We here focus on Bayesian treatment of MLMs, though multilevel modeling is an area where there has been significant cross-fertilization between Bayesian and frequentist approaches. We begin by describing a very simple MLM—the *normal-normal* MLM—highlighting a feature of MLM point estimates—shrinkage—that has connections to classic astronomical approaches for correcting for survey biases. We use this as a stepping stone to a more thoroughgoing Bayesian approach that moves beyond point estimates and corrections. Until recently this approach has been implemented only in fairly simple astronomical settings; we end by highlighting directions for future research.

3.1 Adjusting member estimates: shrinkage

Suppose we have survey data for a population of objects that we will model as having a log-normal luminosity function, so the population distribution of absolute magnitude, M , is a normal distribution with location M_0 and scale (standard deviation) τ (these are the hyperparameters). As a simple starting point, we will suppose τ is known ($\tau = 0.5$ mag, say), and we denote the population distribution by $f(M|M_0)$. For now, we also assume there are no selection effects. At the population level, our goal is to infer M_0 .

The survey produces data, D_i , for each object; we will suppose these lead to independent, Gaussian-shaped likelihood functions for each object’s unknown true abso-

lute magnitude M_i , with maximum likelihood estimates (MLEs) \hat{M}_i and uncertainties (standard deviations) σ_i . We denote these *member* or *object likelihood functions* as

$$\ell_i(M_i) \equiv p(D_i|M_i) = N(M_i|\hat{M}_i, \sigma_i^2), \quad (8)$$

with $N(\cdot|\mu, \sigma^2)$ the normal distribution with mean μ and variance σ^2 . The M_i are the lower level parameters. The survey catalog consists of a table of the \hat{M}_i estimates and their uncertainties, understood here as descriptions of member likelihood functions. For simplicity, we assume equal uncertainties, $\sigma_i = \sigma = 0.3$ mag.

Let $\mathbf{D} \equiv \{D_i\}$ and $\mathbf{M} \equiv \{M_i\}$ denote the collections of data and object parameters, respectively. The likelihood function for the population parameter, M_0 , and all of the latent member parameters, \mathbf{M} , is

$$\mathcal{L}(M_0, \mathbf{M}) \equiv p(\mathbf{D}|M_0, \mathbf{M}) = p(\mathbf{D}|\mathbf{M}) = \prod_i \ell_i(M_i). \quad (9)$$

Note that it does not depend on M_0 because the probabilities for the source data, D_i , are fully determined (and independent) if \mathbf{M} is specified. Thus the joint MLEs for the source parameters are just the independent MLEs: $\hat{\mathbf{M}} = \{\hat{M}_i\}$. But in a Bayesian calculation, estimates are determined by the posterior, not the likelihood. If M_0 is known, the joint posterior for the object parameters, conditional on M_0 , is given by

$$\pi(\mathbf{M}|\mathbf{D}, M_0) \propto \prod_i f(M_i) \ell_i(M_i), \quad (10)$$

with the population density appearing as a prior factor for each source. Point estimates may be found from this conditional posterior, e.g., by finding the mode or posterior mean for \mathbf{M} . It is important to note that if we increase the amount of survey data by increasing N , such Bayesian estimates will *not* converge to the MLEs, because additional prior factors enter with each new source. That is, we are not in the common, simpler setting of a fixed number of parameters, with additional data providing likelihood factors that eventually overwhelm a single prior factor. The presence of member-level uncertainties implies that each new object *adds a new parameter*, so differences between Bayesian and likelihood estimates persist. This is evident in the Malmquist corrections described above. The only way for these Bayesian estimates to converge to MLEs is to add follow-up data for each source, i.e., to make all of the $\ell_i(M_i)$ functions narrower.

Considering the population parameter M_0 to be unknown, with prior distribution $\pi(M_0)$, the joint posterior for all the unknowns is given by

$$\pi(M_0, \mathbf{M}|\mathbf{D}) \propto \pi(M_0) \prod_i f(M_i|M_0) \ell_i(M_i). \quad (11)$$

If our goal is to estimate the source parameters, we account for M_0 uncertainty by marginalizing over M_0 , giving the source parameter marginal posterior, $\pi(\mathbf{M}|\mathbf{D}) = \int dM_0 \pi(M_0, \mathbf{M}|\mathbf{D})$. If instead our goal is to infer the population density, we calculate the marginal posterior for M_0 , $\pi(M_0|\mathbf{D}) = \int d\mathbf{M} \pi(M_0, \mathbf{M}|\mathbf{D})$. In this simple normal-normal MLM, these integrals can be done analytically (we adopt a flat prior for M_0 —the *hyperprior*).

The top panel of figure 2 shows the PDF for a population distribution with $M_0 = -21$; the circles on the line just below it indicate the true M_i values of a sample of $N = 30$ objects. Below that, diamonds indicate the MLEs for the objects, \hat{M}_i , for one realization of measurement error; a line segment connects each estimate with its true parent value. The MLEs are intuitively appealing estimates; they also have several appealing frequentist properties, considering an ensemble of many realizations of the measurement errors for a particular object. For example, normal MLEs are unbiased (in fact, they are the best linear unbiased estimators), and they are invariant to translation in M . But considered as an ensemble, they are overdispersed with respect to the population distribution; this is visually evident in the figure. Intuitively, the MLEs here can be viewed as samples from a modified population density that is the convolution of the true population density with the error density (though we note that this convolution interpretation does not generalize to more complicated settings).

As alternatives to the MLEs, consider Bayesian estimates, in two different scenarios. First, suppose we knew $M_0 = -21$ a priori. Using the (known) population distribution as the prior for each M_i produces posteriors that remain independent and normal, but with means, \tilde{M}_i , shifted from the MLEs toward M_0 . Define $b \equiv \frac{\sigma^2}{\sigma^2 + \tau^2}$; then the posterior means (and modes) are given by

$$\tilde{M}_i = (1 - b) \cdot \hat{M}_i + b \cdot M_0, \quad (12)$$

and the variance for each estimate is reduced to $(1 - b)\sigma^2$ rather than just σ^2 . The squares on the third line below the panel in figure 2 show these estimates. They all move toward M_0 , and thus toward each other. One says that the ensemble of estimates “shrinks toward M_0 ,” this phenomenon is called *shrinkage*. They are labeled “Cond” in the figure to indicate that we conditioned on M_0 .

As an ensemble, the shrunken estimates look more like the true values than the MLEs. These estimates are biased and are no longer invariant, but even from a frequentist perspective they may be deemed better than the MLEs: despite the bias, the shrunken estimates are, on the average (over error realizations, and across the population), closer to the true values than the MLEs—i.e., they have smaller mean squared error (MSE)—as long as $N > 2$. Stein discovered this effect around 1960, and after a decade or two of sorting out its subtleties, the use of deliberately (and carefully) biased estimators for joint estimation of related quantities is now widespread in statistics (frequentist and Bayesian), and considered one of the key innovations of late-20th century statistics.

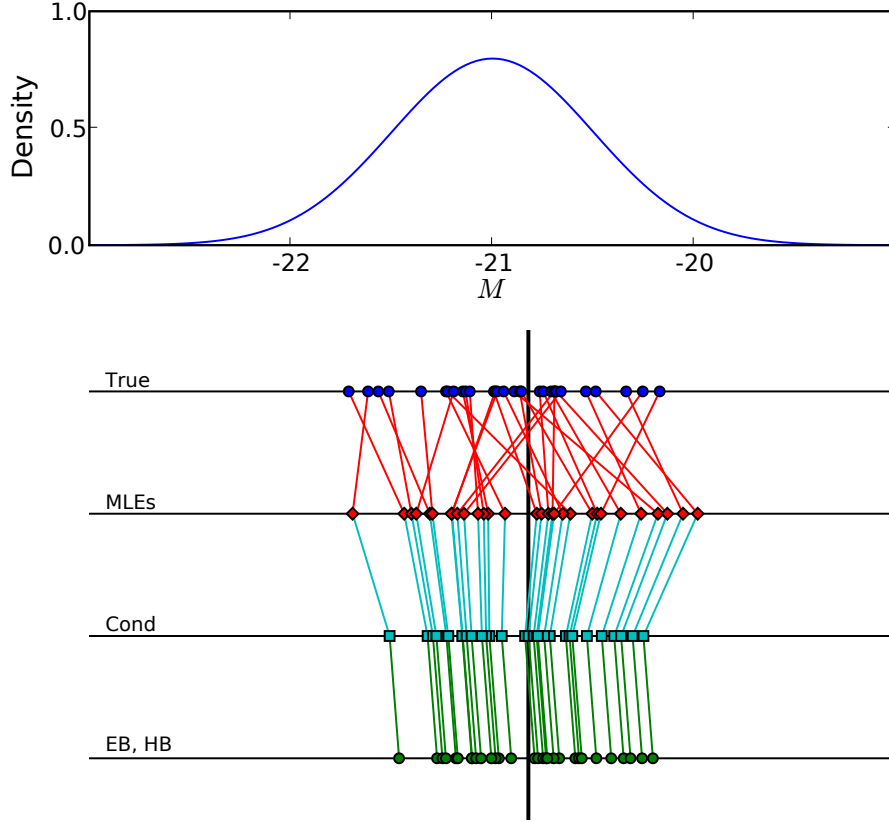


Figure 2: Shrinkage in a simple normal–normal model. Top panel shows population distribution; “True” axis shows M_i values of 30 samples. Remaining axes show estimates from measurements with $\sigma = 0.3$ normal error: MLEs, conditional (on the true mean), and empirical/hierarchical Bayes estimates.

We have used strong prior information here—precise knowledge of M_0 . But what if we did not know M_0 a priori? The *empirical Bayes* (EB) approach “plugs in” an ad hoc estimate of M_0 and uses the resulting prior. The obvious estimator here is \bar{M} , the average of the MLEs, whose position is indicated by the thick vertical line in the figure. Using the resulting prior produces the circle estimates on the bottom axis, still shrunk, but towards \bar{M} rather than M_0 . Equation (12) again gives the estimates, if we replace M_0 with \bar{M} . Note that since \bar{M} depends on *all* of the MLEs, the EB estimates are *no longer independent*.

From a fully Bayesian point of view, plugging in \bar{M} for M_0 is unjustified; M_0 is unknown, so we should consider it a parameter, assign its prior distribution, and marginalize over it, an approach called *hierarchical Bayes* (HB). The resulting estimates are identical to the EB estimates in this problem (though they need not be in

general); however, the uncertainties in the HB estimates are somewhat larger than those produced in an EB calculation, reflecting uncertainty in the shrinkage point. We have motivated EB and HB shrinkage estimates via Bayesian arguments, but the frequentist advantages of shrinkage in the conditional case still hold: despite their bias, as a group these estimates have smaller MSE than the MLEs. In addition, due to their accounting for M_0 uncertainty, confidence intervals based on the HB procedure have more accurate frequentist coverage than EB intervals (Carlin and Louis 2000).

The conditional shrinkage estimates are the normal-normal model counterparts to homogeneous Malmquist and Lutz-Kelker corrected estimates (the latter do not so obviously “shrink” because the prior in astronomical settings is much broader than a normal distribution). On the one hand, this is a source of comfort, in that some of the statistical benefits of shrinkage are presumably shared by the astronomical methods. However, the correspondence is also a source of caution and concern. Decades of study have revealed shrinkage to be a subtle phenomenon, with snares for the unwary. We highlight just a few key developments here; entries to the large literature in this area include Carlin and Louis (2000), Carlin et al. (2006), and Browne and Draper (2006).

Most obviously, as noted in Section 2.2, the homogeneous density assumption of the classic corrections is seldom justifiable; in reality, the population density is inhomogeneous—and unknown. That is, conditional shrinkage is not appropriate; something along the lines of the EB or HB approaches is in order. This must be done with some care: it is known that shrinkage may not improve estimates, and may even worsen them, if done in a matter that does not reflect the true distribution of lower level parameters. The EB approach—using a “plug-in” estimate of hyperparameters to specify the population hyperprior—has appealing simplicity; the Landy-Szalay approach probably has an approximate EB justification. But it is known that EB approaches tend to underestimate final uncertainties (due to ignoring hyperparameter uncertainty). HB estimates can offer improvements, but with computational costs, and with other challenges noted below.

More subtly, shrinkage must be tuned, not only to the underlying population distribution, but also to the *inferential goal*. The shrinkage estimates just described do indeed reduce the MSE of the collection of source absolute magnitudes. But if one uses the shrunken point estimates to infer the population distribution, it turns out the point estimates are *underdispersed* and the distribution may be poorly estimated. If one instead seeks from the beginning point estimates that are optimal for estimating the population distribution (via a decision-theoretic calculation), a different shrinkage prescription is appropriate. Similarly, it is evident from the segments connecting the true M_i ’s with their MLEs that the ranks of the sources are shuffled, and shrinkage has not corrected it. In some settings, shrinkage estimates that improve rank estimates have been identified; they differ from those optimal for individual parameter

or distribution estimates. There is a kind of “complementarity” in relying on point estimates for subsequent inferences; estimates optimal for some questions may be misleading for other questions (Louis 1984).

A main source of these complications is the inadequacy of point estimates as summaries of a correlated, high-dimensional posterior distribution. This motivates a more thoroughly Bayesian treatment in the spirit of HB, relying on marginalization over uncertain parameters rather than use of point estimates. We pursue this approach below.

But before doing so, some comments at a conceptual level are appropriate here. The second level of our MLM here describes the population with a continuous density. A frequentist interpretation of this density is problematic. The volume accessible to a survey—indeed, the volume within the horizon—contains a finite number of sources (galaxies, clusters, quasars, gamma-ray bursts, etc.). Repeating a survey will produce catalogs that largely contain the same sources (some sources near the survey detection limit may differ from one repetition to the next); the population density cannot be interpreted in terms of frequentist variability. At the lower level of the MLM, measurement errors may differ among repetitions, but if the lower level uncertainties are the result of indicator scatter—itself a population-level phenomenon—lower-level results will also be the same across repeated surveys.

From the Bayesian point of view, the population PDF describes a priori *uncertainty* about the value of a property for a population member, not (directly) *variability* in repeated sampling; its introduction and specification should be motivated by epistemological considerations. One way to formally motivate it is as a mechanism to introduce dependence among estimates. That is, we expect that learning the properties of many objects of a particular type should help us predict the properties of as-yet unmeasured objects of that type; this is what it means to consider the objects to comprise a population. Consistency requires that, once we obtain measurements of new objects, we cannot ignore the prior information provided by measurements of other objects that we would have used in the absence of the data. The resulting dependences in the joint posterior pools information, leading to shrinkage.

More formally still, we might justify introducing a population density by requiring the joint prior distribution for a set of object properties to be *exchangeable*, that is, invariant to permuting the labels of objects. E.g., in the setting above, $p(M_1, M_2, \dots, M_N | \theta)$ should take the same functional form if we permute the order of the $\{M_i\}$. This appears to be both a natural and a weak assumption. It is in the spirit of the common “IID” (independent and identically distributed) assumption in that the marginals for each source are identical; but by allowing dependence, it sets the stage for sharing of information across the population. Surprisingly, *exchangeability itself implies the hierarchical Bayes structure*: the (continuous) de Finetti exchangeability theorem implies that any such exchangeable distribution can be written as a

density-weighted mixture of identical, conditionally independent distributions, i.e., as a hierarchical Bayesian model. In the setting here, the theorem says one may write

$$p(M_1, M_2, \dots, M_N) = \int d\theta \mu(\theta) \prod_i f(M_i|\theta), \quad (13)$$

where $\mu(\theta)$ defines a unit-normed measure over θ , specifying the form of the independent densities $f(\cdot|\theta)$. The theorem is a purely mathematical result providing a representation for symmetric functions, but in a Bayesian context it motivates introducing a continuous population density, playing the role of $f(\cdot)$, with a hyperprior playing the role of μ .³

3.2 Thinned latent marked point process models

While the MLM setup above has the essential ingredients needed for us to move beyond point estimate-based population modeling, we need to generalize it in two ways to meet the needs of astronomical survey analysis. First, the analysis above took the catalog size, N , as given. In an astronomical survey, N is instead determined by the population density and the volume surveyed; it is thus informative about the population. Second, astronomical surveys suffer from selection effects, most typically in the form of thinning or truncation in a “blind,” “ab initio,” or “blanket” survey (where sources may be missed due to detection criteria), or censoring in a targeted follow-up survey (where sources known to exist may have unmeasurable properties due to limited sensitivity). We discuss the thinning/truncation case here.

To allow catalog size to be informative about the population density, we model the population with an inhomogeneous (marked) Poisson point process, characterised by an *intensity function* rather than a probability density function. The Appendix develops this model in detail; here we outline its main features. Let \mathcal{O} denote the per-object latent parameters specifying properties of interest for an object (e.g., flux, redshift, luminosity, size, morphology, etc.). The Poisson point process assumption implies there is an intensity function, $\mu(\mathcal{O})$ that, when known, allows us to write the probability for there being an object with \mathcal{O} in the interval $[\mathcal{O}, \mathcal{O} + d\mathcal{O}]$ as $\mu(\mathcal{O})d\mathcal{O}$, to leading order in \mathcal{O} . It also presumes that this probability is independent of whether an object is found in any other (distinct) interval (provided we know the intensity $\mu(\cdot)$; i.e., this is *conditional* independence). Usually we will not know the intensity, e.g., it may depend on parameters, θ , whose values are uncertain, which we indicate by writing $\mu(\mathcal{O}; \theta)$.

³Rigorously, the theorem requires that the judgement of exchangeability apply for any selection of a finite set of M_i ’s from an infinite set. If there is a finite limit to N , the integral representation may not be able to represent some possible exchangeable distributions, though the restriction is minor if the limit is large. See Diaconis and Freedman (1980) for details.

To account for (random) truncation, we introduce a survey detection efficiency, $\eta(\mathcal{O})$, specifying the probability that an object with parameters \mathcal{O} will be detected. Although we take $\eta(\mathcal{O})$ as given in what follows, it is worth noting (especially for non-astronomer readers) that calculating the η which characterises a particular survey is often a very difficult task, requiring both careful measurement and calibration, and often extensive Monte Carlo simulation. Not all surveys provide an accurate detection efficiency, yet it is necessary for what follows. (In some cases it may be possible to partially infer η from the available survey data; we do not cover this somewhat subtle task here.)

Finally, we highlight a point made in passing above: from the Bayesian point of view, a survey catalog should not be viewed as providing *estimates* of object properties, but rather as providing summary statistics specifying *member likelihood functions*, $\ell_i(\mathcal{O}_i) = p(D_i|\mathcal{O}_i)$, where D_i denotes the data for object i . This change in viewpoint has far-reaching implications. It can enable more accurate accounting of object uncertainties, e.g., by reporting a likelihood parameterisation more complex than the traditional “best-fit \pm uncertainty,” such as a parameterisation describing possible likelihood skewness (as might be important near detection limits). It also opens the door to use of marginal detections or upper limits in censored surveys, by averaging over object uncertainties with likelihoods that are significantly non-Gaussian, possibly peaking at zero object flux.

With these ingredients in hand, one can calculate the thinned latent Poisson point process counterpart to the MLM joint posterior density for the population and source parameters of equation (11) (see Lored & Wasserman 1995 or Lored 2004 for early derivations; a more thorough and general treatment is in the Appendix):

$$\pi(\theta, \{\mathcal{O}_i\}|D) \propto \pi(\theta) \exp \left[- \int d\mathcal{O} \eta(\mathcal{O}) \mu(\mathcal{O}; \theta) \right] \prod_{i=1}^N \ell_i(\mathcal{O}_i) \mu(\mathcal{O}_i; \theta). \quad (14)$$

Marginal posteriors for θ or $\{\mathcal{O}_i\}$ may be calculated as was done above, though obviously the calculations can be challenging for astrophysically interesting models. Our own applications to date have been to situations with parametric population models, where \mathcal{O} was one-dimensional (magnitudes of trans-Neptunian objects (TNOs); Petit et al. (2007) and references therein), or three-dimensional (fluxes and directions of gamma-ray bursts; Lored & Wasserman 1998a,b). In these cases the N integrals over \mathcal{O}_i were done by quadrature.

As a simple example focusing on one aspect of the MLM approach—the value of marginalizing over source uncertainty—consider a magnitude survey (i.e., the “number counts” setting), where $\mathcal{O} = m$, the apparent magnitude of a source. Suppose the source population has a rolling power law distribution of fluxes, so we may write the magnitude distribution as $\mu(m) = A \times 10^{[\alpha(m-23) + \alpha'(m-23)^2]}$, where A is the density per unit magnitude at $m = 23$, and α and α' give the slope of the number-magnitude

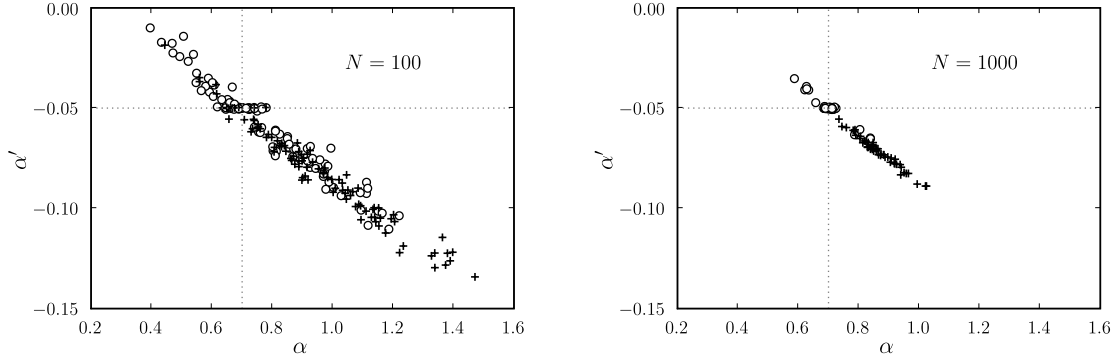


Figure 3: Scatter plots of posterior modes for population parameters, using data simulated from a rolling power law, from a Bayesian analysis marginalizing over source parameters (circles), and a maximum likelihood analysis using best-fit source estimates (+ symbols). Left panel is for simulated surveys of $N = 100$ sources; right panel is for $N = 1000$.

distribution, and its rate of change with m , at $m = 23$. We simulated sources from this distribution, and simulated detections and measurements for a very simple survey performing source detection and measurement via photon counting. The survey parameters were chosen so that the dimmest detected sources have magnitude uncertainties ~ 0.15 magnitudes. We analysed data from many simulated surveys, all of a population with $\alpha = 0.7$ and $\alpha' = -0.05$ (values that describe some TNO data), and estimated α and α' by finding the mode of the marginal posterior for these parameters, marginalizing equation (14) over all the latent m_i parameter, and the amplitude, A . The resulting (α, α') estimates, for surveys of size $N = 100$, are plotted as the open circles in the left panel of figure 3; the crosshair shows the true parameter values. We also calculated maximum likelihood estimates of α and α' , maximizing the full joint likelihood also over the latent parameters, i.e., using only the best-fit m_i estimates (not marginalizing). These are plotted as “+” symbols in the figure. The Bayesian estimates are distributed roughly symmetrically about the truth; the MLEs are clearly biased toward large α and small α' , though the uncertainties are large enough that the estimates are sometimes accurate.

The right panel shows results from the same calculation, but with $N = 1000$. The Bayesian estimates have converged closer to the truth. In contrast, the MLEs have converged *away* from the truth. This example highlights the value of marginalization, particular in settings with measurement error. In such settings, each new object adds its member parameter(s) to the problem; one is not in the fixed parameter dimension setting in which our statistical intuitions about “root- N convergence” are trained. As a result, the effects of object uncertainties do not “average out;” instead, it becomes *more* rather than less important to carefully account for them as survey size grows. This aspect of population modeling has been repeatedly rediscovered by astronomers.

The earliest discovery we know of is Eddington’s treatment of what has become known as *Eddington bias* (Eddington 1940). A recent rediscovery in a cosmological context is Sheth’s work on the effects of photometric redshift errors on modeling galaxy and quasar populations (Sheth 2007). Sheth advocates an ad hoc deconvolution algorithm; we think hierarchical Bayes offers a vastly more flexible and accurate framework for addressing such problems.

4 Research directions

Fully Bayesian hierarchical modeling of cosmic populations is challenging. Most applications to date either rely on fairly simple models, or, when considering complex models, consider small or modest-sized surveys. The earliest HBM work in cosmic demographics appears to be the work of Loredo & Wasserman (1995, 1998a,b) on gamma-ray burst (GRB) demographics; they adopt parametric number-counts and luminosity function models for samples of $\sim 10^3$ GRBs. The challenging VELMOD analysis of Tully-Fisher data by Willick and Strauss 1998, mentioned in Section 2.3, includes many key elements of hierarchical Bayes, but does not implement a fully Bayesian calculation. The state-of-the-art for large-scale multilevel modeling of survey data is probably the reanalysis of the Sloan Digital Sky Survey (SDSS) catalog by Regier et al. (2019), but this calculation adopts fixed population distributions, and invokes strong approximations to enable large-scale computations using a variational inference algorithm. See Loredo (2013) for a recent survey of hierarchical Bayesian modeling of cosmic populations. Future research must explore applications of increased complexity in three different dimensions: survey size, source parameter dimension, and population model complexity.

An obvious need is development of numerical algorithms appropriate for multivariate observables and large surveys, perhaps invoking approximations or using Monte Carlo methods and parallel computing for member latent parameter marginalization (see Szalai-Gindl et al. 2018 for promising work along these lines using GPUs to implement parametric HBMs for population sizes $\sim 10^6$, with low-dimensional member properties). With respect to multivariate observables, it will be insightful to work out the detailed connections between the MLM approach and other methods, such as those surveyed in Section 2. For example, when the observables are flux and a distance indicator, an analogue to the direct indicator method should “fall out” of an MLM calculation when the source likelihoods provide precise estimates of the indicators.

Implementing Bayesian MLM with more complex population models will also demand development of clever algorithms. But more subtle and interesting challenges arise as model complexity increases. These challenges arise because of the “softening” of the impact of member-level measurements on inferences, due to uncertainties. We saw above that this “changes the rules” in the sense of causing violations of naive

intuition about uncertainties averaging out as N grows. But this is only one of several issues complicating life with multilevel models.

Some of these issues mimic problems associated with nonparametric modeling, and this is no accident. Though a common informal “definition” of nonparametric model is a model with an infinite number of parameters, a more insightful definition is a model in which the *effective* dimension of the parameter space can grow with sample size. In fact, the “many normals” problem—essentially the normal–normal MLM, with the actual dimension growing linearly with sample size—is sometimes used as a surrogate for more complex nonparametric models in theoretical analyses (e.g., Wasserman 2005).

A prime issue which nonparametric modellers must face is assessing how priors over large-dimensional spaces may influence inferences. Similar concerns arise for MLMs. For example, for estimating the mean and standard deviation of a normal distribution using *precise* measurements, common default priors are flat for the mean and log-flat for the standard deviation. We saw above that a flat prior for M_0 in the normal–normal MLM produced sensible inferences. But had we considered the population standard deviation τ to be unknown, we would have discovered that a log-flat τ prior leads to an improper (unnormalisable) posterior. Instead, priors flat in τ or τ^2 (among others) are advocated, with various justifications (sometimes including the good frequentist performance of the resulting estimates; see, e.g., Berger et al. 2005; Gelman 2006). This indicates that as astronomers increase the complexity of MLMs for surveys, care must be taken with priors; statisticians have helpful insights to offer here. It also suggests that model checking, in the spirit of goodness-of-fit tests, is important for MLMs. Their rich structure makes conventional model checking methods inappropriate, but there is useful research on model checking methods tailored to MLMs (e.g., Sinharay & Stern 2003; Bayarri & Castellanos 2007).

An alluring direction for increasing model complexity is to make the population model itself truly nonparametric. One motivation comes from existing nonparametric methods designed to flexibly account for selection effects, such as the C^- method of Lynden-Bell (1971) or the stepwise maximum likelihood method (Efsthathiou et al. 1988). These methods ignore object uncertainties; finding counterparts in the MLM framework promises to broaden applicability of such approaches, and unify them with approaches relying on Malmquist-style corrections (insofar as MLMs have shrinkage “built in”). But the fact that *parametric* MLMs already have some of the issues of nonparametric modeling suggests that nonparametric multilevel modeling will be tricky, requiring even more care with assessing robustness to priors. Fortunately, there are successful examples in the statistics literature to build upon (e.g., Müller & Quintana 2004).

Sensitivity to priors can make newcomers to Bayesian methods consider retreating to frequentist territory. But there is little solace there; the subtleties of complex mul-

tilevel Bayesian modeling reflect genuine complexity in the task of modeling surveys, complexity that has frequentist implications. For example, the best-studied methods for nonparametric analysis of survey data with uncertainties (yet to be extended to include truncation) rely on deconvolution. Though the methods are straightforward, it is known that the resulting population estimates have discouragingly slow rates of convergence (often only logarithmic in N , as opposed to the \sqrt{N} we are accustomed to for parametric inference without measurement errors; see Loredo 2007 for discussion and entries to the literature). In fact, leading developers of such methods have recently turned to Bayesian methods, where careful attention to structure in the prior can lead to methods with improved performance (e.g., Berry et al. 2002).

We think development of *semiparametric* population models for use in MLM analyses of survey data may be an especially fruitful research direction. For example, we envision nonparametric modeling of the density distribution of galaxies, combined with parametric modeling of the luminosity function (e.g., by a Schechter function or a mixture of a few Schechter functions), as a promising approach, allowing adaptivity to complex spatial structure, but hopefully providing good convergence rates for learning the luminosity function. But there are several challenges to conquer on the path from the current state of the art to such a goal.

We are grateful to many collaborators and colleagues who have contributed to our understanding of survey biases and population modeling, especially David Chernoff, Woncheol Jang, David Ruppert, John Simmons, and Ira Wasserman. We also gratefully acknowledge the Statistical and Applied Mathematical Sciences Institute (SAMSI), whose 2006 Astrostatistics Program and 2016 ASTRO Program assembled astronomers and statisticians to discuss these issues. Loredo was partly supported by NSF grant AST-0507589 and by NASA grants NAG5-12082 and NG06GH84G for work reported here. Both Loredo and Hendry were supported by NSF grant AST-1312903 for work described in the appendix.

Appendix: Thinned latent marked point process likelihood function

In this Appendix we derive the likelihood function for the parameters of a population model and the population’s latent parameters, presented as equation (14) in § 3.2. As noted there, this likelihood function is based on catalog data describing member likelihood functions for detected objects, and appropriate summaries of the detection criteria to account for selection effects; here we describes those features in more detail. For concreteness, we treat the case of using galaxy survey data to infer a luminosity function. The latent object parameters are flux, direction (or 2D position on the detector), and distance, $\mathcal{O}_i = (F_i, x_i, z_i)$. For simplicity, we treat the case where

the data provide noisy flux estimates, but where redshift is precisely known (e.g., considering a sample that supplements photometry with high-resolution spectroscopy with good signal-to-noise).

Object detection is typically implemented via a scanning procedure. For example, for image data, a fixed aperture may be scanned over the image. As the scan proceeds, a detection algorithm determines if an object is present at each candidate location, e.g., by comparing the estimated flux in the aperture to a threshold value (set by background and noise estimates), or by fitting an image model to the data in the aperture and comparing the fitted amplitude to a threshold. For time series data, a window may be scanned over the time series, with an object detected if the estimated flux in the window is above a threshold. If an object is detected, its properties are more carefully estimated, e.g., by a likelihood-based or weighted least-squares calculation, with estimation results summarized in the catalog.

Fig. A.4 illustrates the process and its relationship to catalog construction. We split the object property parameter space into *scan* and *mark* components. The scan component corresponds to the dimensions over which the detection scan operates; the mark component corresponds to the remaining dimensions. For our galaxy luminosity function example, the scan component is the two-dimensional position of the galaxy image on the detector (corresponding to its direction on the sky), and the mark component is the galaxy luminosity and distance, or equivalently, flux and distance (in a more complex case, the mark component might include color and morphological parameters). In the figure, the dots (red) indicate the true properties of seven galaxies; the blue contours depict likelihood functions for the properties, based on noisy image data (the displayed contours are from simulations using a simple 1-D image model, with a single location parameter, and a flux parameter). The gray region at the bottom is bounded above by the position-dependent detection threshold; an object is detected only if its best-fit (maximum likelihood) flux is above the threshold. The region is depicted with a gradient to depict that, as a function of *true* object properties, the resulting selection is probabilistic. Here two of the seven objects are not detected.

We model the properties using a (latent) marked Poisson point process, i.e., a Poisson point process for the scanned parameters, and a probability density function for the mark parameters. For concreteness, we focus on the luminosity function example, taking the scan parameter to be object position, x (a 2D parameter, e.g., direction on the sky), and the mark parameters to be flux and distance, (F, r) . We suppose that the spatial density of galaxies is approximately constant over the region probed by the survey. There is thus a constant Poisson intensity parameter, λ , specifying the density of galaxies in x . We assume a luminosity PDF that is independent of distance (of course, the flux PDF will depend on distance, thanks to the inverse square law). The flux and distance mark PDF is thus a product of a distance PDF, $h(r)$, and a

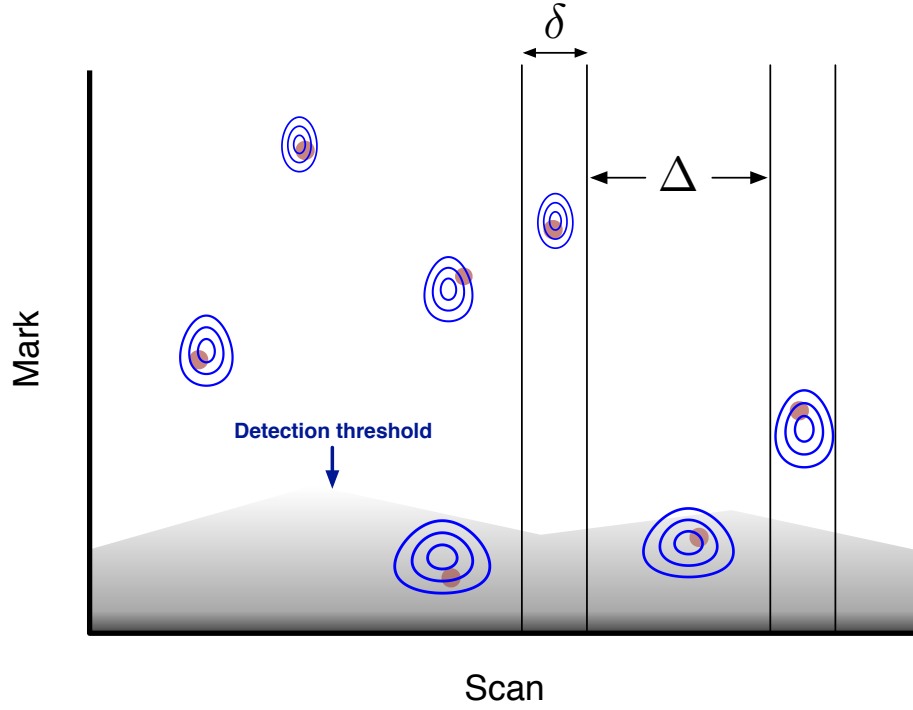


Figure A.4: Depiction of thinned latent marked point process model for catalog data produced by an astronomical survey. Object properties are split into a scanned subset and a mark subset. Dots (red) show latent (true) values for an object's properties. Contours (blue) depict member likelihood functions from analysis of the raw survey data; catalogs provide summaries of these for detected objects. Gray region at bottom depicts the non-detection region; candidates with estimated mark values below a varying threshold are rejected. δ and Δ denote sizes of example detection and nondetection intervals.

conditional flux PDF, $\rho(F, r)$. We use ζ to denote the flux PDF parameters, writing it as $\rho(F, r; \zeta)$ when we want to display the parameter dependence.

For the PDF for galaxy distance, $h(r)$, we assume homogeneity, which implies

$$h(r) = \begin{cases} \frac{3r^2}{r_u^3} & \text{if } 0 \leq r \leq r_u, \\ 0 & \text{otherwise,} \end{cases} \quad (\text{A.15})$$

where r_u is an upper limit on distance chosen to be beyond the surveyed volume. (That is, r_u is chosen so that the most luminous galaxies of interest have fluxes comfortably below the lowest flux threshold. In deep surveys, reaching to very dim fluxes, cosmological considerations, including the finite age of the universe and the non-Euclidean geometry of spacetime, ameliorate the growth of $h(r)$ with r .) The population model thus has parameters $\theta = (\lambda, \zeta)$.

We consider a case where we have precise distance measurements for the galaxies (e.g., from high-resolution spectroscopic data providing precise redshifts). We assume independent errors in the position and flux measurements, so the catalog contains descriptions of separate member likelihood functions for flux and position, denoted $\ell_i(F)$ and $m_i(x)$ for galaxy i , with $i = 1$ to N .⁴ Formally, denoting the image data for detected galaxy i by D_i , we are writing

$$p(D_i|x, F, r) = \ell_i(F) m_i(x) \delta(r - r_i), \quad (\text{A.16})$$

where the Dirac delta function factor represents the precise measurement of distance.

We must also describe the survey’s selection effects. These are determined by the detection threshold as a function of the scan location. At each scanned location, x , the threshold determines the set, \mathcal{D}_x , of possible data (i.e., arrangements of counts in the pixels in a scanned aperture) that would pass detection criteria. For example, if the detection criterion is that the MLE flux estimate, $\hat{F}(D)$ for data D , must exceed a threshold $F_{\text{th}}(x)$, then $\mathcal{D}_x = \{D : \hat{F}(D) > F_{\text{th}}(x)\}$. Reporting \mathcal{D}_x , or equivalently $F_{\text{th}}(x)$, then describes the selection effects. But we will see below that a more compact summary of the detection criteria will be more convenient.

We now compute the likelihood function for the parameters, based on catalog data describing member likelihood functions and the selection effects. For simplicity, we here consider “nearly-pure catalog” settings with stringent detection criteria (e.g., high thresholds), so that it is unlikely there are any false detections in the catalog (it is straightforward to generalize to settings with nonnegligible false detection rate). Fig. A.4 includes depictions of elements of our construction. We partition the scan

⁴Independence of flux and position estimates is almost universally assumed for astronomical catalogs, but for dim sources there can be significant dependence. We depict this in Fig. A.4.

space into N detection intervals, δ_i , containing a single detected object, and M non-detection intervals, Δ_j , in which no candidate object passed the detection criterion.⁵ The likelihood function is the product of the (conditionally independent) probabilities for these intervals.

We first consider the probability for no detection in one of the Δ_j intervals. We break it up into subintervals of size δx , small enough that the detection threshold is approximately constant over the interval. The probability for seeing no detections in δx is the sum of the probabilities for the following events (conditioned on the population parameters, (λ, ζ)):

- No objects have x in the interval.
- One object has x in the interval, but it produced data that were not in \mathcal{D}_x .
- Two objects have x in the interval, but both produced data that were not in \mathcal{D}_x .
- And so on. . . .

Each event is a conjunction of two simpler events, the Poisson probability for the specified number of objects lying in the interval, and the probability for not detecting any events in the interval. We will express the latter probability in terms of the *detection efficiency* at x for objects with flux F ,

$$\eta(x, F) \equiv p(D \in \mathcal{D}_x | F) \quad (\text{A.17})$$

$$= p(\hat{F}(D) > F_{\text{th}}(x) | F), \quad (\text{A.18})$$

where F as a conditioning symbol signifies that an object is present with flux F . The probability for detecting an object with unspecified flux and distance, given the population parameters, is then

$$p_x(\zeta) = \int dr \int dF \rho(F, r) h(r) \eta(x, F). \quad (\text{A.19})$$

The probability for *not* detecting an object with a given location is then $1 - p_x(\zeta)$.

Now let ν denote the (unknown) number of objects with x in δx . Then the probability for no detections in δx at x is

$$\begin{aligned} q(x) &= \sum_{\nu=0}^{\infty} \frac{(\lambda \delta x)^\nu}{\nu!} e^{-\lambda \delta x} [1 - p_x(\zeta)]^\nu \\ &= e^{-\lambda \delta x} \sum_{\nu=0}^{\infty} \frac{(\lambda \delta x)^\nu [1 - p_x(\zeta)]^\nu}{\nu!} \\ &= \exp[-\lambda \delta x p_x(\zeta)]. \end{aligned} \quad (\text{A.20})$$

⁵We are presuming that galaxy images are well-separated, i.e., we do not treat here the *crowded field* or *strongly blended* case, where the images of distinct objects may strongly overlap.

This is the probability for no detections in a subinterval of a Δ_j interval. The probability for no detections across the entire interval is the product of its subinterval probabilities. The exponents add, comprising an integral over the Δ_j intervals, so that the nondetection probability becomes

$$q(\Delta_j) = \exp \left[-\lambda \int_{\Delta_j} dx \int dr \int dF \eta(x, F) h(r) \rho(F, r) \right]. \quad (\text{A.21})$$

This is just the Poisson probability for seeing no events, when the expected number of events is λ times the fraction of the population expected to be detected in the interval, given the threshold behavior (encoded in the detection efficiency).

Now consider the probability for the data associated with a detection interval, δ_i ; for simplicity, we assume all of these intervals are of the same size, δ , in x . The probability for getting data D_i from detection of an object in δ_i is the sum of the probabilities for the following events:

- One object has x in the interval, and was detected producing data D_i .
- Two objects have x in the interval, one of which was detected producing D_i , with the other undetected.
- And so on. . . .

To simplify the calculation, let us stipulate that the detected object has values of (x, F, r) known precisely, i.e., lying in small intervals (dx, dF, dr) ; at the end, we will account for their uncertainty via marginalization.

The first case is simple; the probability for one object in the interval, having the specified properties, and being detected producing D_i , is

$$p_1(\lambda, \zeta) = (\lambda\delta) e^{-\lambda\delta} \left[\frac{dx}{\delta} h(r) dr \rho(F, r; \zeta) dF \right] p(D_i \in \mathcal{D}_x, D_i | x, F, r). \quad (\text{A.22})$$

The final probability factor here is for a conjunction; it may be written

$$p(D_i \in \mathcal{D}_x, D_i | x, F, r) = p(D_i | x, F, r) p(D_i \in \mathcal{D}_x | D_i), \quad (\text{A.23})$$

where we have dropped (x, F, r) from the last factor because the values of the properties are irrelevant for determining detection, once the data are in hand. Now note that detection is deterministic given the data, i.e., either the data correspond to a candidate passing the detection criteria or not. But for a detected object, by definition the data passed the criteria, so the last factor is equal to unity. The first factor we recognize as the member likelihood function, defined in (A.16). This completes the computation of $p_1(\lambda, \zeta)$.

For cases with $\nu > 1$ objects present, we will have a factor like $p_1(\lambda, \zeta)$ for the detected object, and nondetection probabilities for undetected objects of the form of the $[1 - p_x(\zeta)]$ factor appearing in the Δ_j probability derived above. But in addition, we have to account for not knowing which of the ν objects is detected. The resulting probability for the case of ν objects present can be written as follows:

$$\begin{aligned}
p_\nu &= \frac{(\lambda\delta)^\nu}{\nu!} e^{-\lambda\delta} \\
&\times \left(\frac{dx}{\delta} h(r) dr \rho(F, r; \zeta) dF \right) \ell_i(F) m_i(x) \delta(r - r_i) \\
&\times [1 - p_x(\zeta)]^{\nu-1} \\
&\times \nu.
\end{aligned} \tag{A.24}$$

Line by line, the factors are:

- the Poisson probability for ν objects being in the interval,
- the probability for one of them having the given properties and producing the detection data, D_i ,
- the probability for the remaining objects not being detected,
- a factor of ν from summing over the possibilities for which of the ν objects is detected.

To facilitate summing the p_ν probabilities over ν , we rewrite (A.24), gathering the ν -dependent terms on the second line of the following equation:

$$\begin{aligned}
p_\nu &= (\lambda\delta) e^{-\lambda\delta} \left(\frac{dx}{\delta} h(r) dr \rho(F, r; \zeta) dF \right) \ell_i(F) m_i(x) \delta(r - r_i) \\
&\times \frac{1}{(\nu-1)!} (\lambda\delta)^{\nu-1} [1 - p_x(\zeta)]^{\nu-1}.
\end{aligned} \tag{A.25}$$

Upon summing over $\nu \geq 1$, and marginalizing over the uncertain values of (x, F, r) , we find that the probability for the detection data in interval δ_i is

$$p(D_i | \lambda, \zeta) = q(\delta_i) h(r_i) (\lambda\delta) \left[\int_{\delta_i} \frac{dx}{\delta} m_i(x) \right] \left[\int dF \rho(F, r_i; \zeta) \ell_i(F) \right], \tag{A.26}$$

where $q(\delta_i)$ is an exponential of an integral, the same function appearing in the nondetection probability of (A.21).

The likelihood function is the product of detection probabilities (A.26) and nondetection probabilities (A.21) for all of the δ_i and Δ_j intervals. All of these probabilities

share an exponential factor resembling (A.21). In the product, there will be a sum of the integrals in the exponents; this corresponds to a single integral over the entire x domain of the survey, of the form:

$$\lambda \int_{\Omega} dx \int dr \int dF \eta(x, F) h(r) \rho(F, r; \zeta), \quad (\text{A.27})$$

where Ω denotes the full range of positions surveyed (which would be measured in terms of solid angle on the sky). Note that the only x -dependent factor in the integrand is the detection efficiency. This lets us write the integral in simpler manner. Introduce the *average detection efficiency*,

$$\bar{\eta}(F) \equiv \frac{1}{\Omega} \int_{\Omega} dx \eta(x, F). \quad (\text{A.28})$$

Using this, (A.27) can be written as a two-dimensional integral,

$$(\lambda\Omega) \int dr \int dF \bar{\eta}(F) h(r) \rho(F, r; \zeta). \quad (\text{A.29})$$

The factor $(\lambda\Omega)$ is the expected number of objects in the surveyed region, which depends only on the λ parameter. The remaining factor is the fraction of these that are detectable; it depends only on the remaining population parameters, ζ .

Equation (A.29) shows that the average efficiency is a kind of sufficient statistic for the survey's threshold behavior. Although catalog builders must determine the detection efficiency over the entire range of the survey, they need only report the lower-dimensional average efficiency for analysts. A common way to compute a survey's detection efficiency is via a Monte Carlo injection study (i.e., injecting simulated objects with known properties into the detection software pipeline). Such studies implicitly do this averaging calculation via Monte Carlo.

We can now write down the full likelihood function for the luminosity function parameters. Dropping some factors that do not depend on the parameters, the likelihood function is

$$\begin{aligned} \mathcal{L}(\lambda, \zeta) = \lambda^N \exp \left[-(\lambda\Omega) \int dr \int dF \bar{\eta}(F) h(r) \rho(F, r; \zeta) \right] \\ \times \prod_{i=1}^N h(r_i) \int dF \rho(F, r_i; \zeta) \ell_i(F). \end{aligned} \quad (\text{A.30})$$

This likelihood function corresponds to equation (14) in the main text, specialized to this luminosity function inference problem.

This likelihood function is reminiscent of that for an inhomogenous Poisson point process, whose likelihood is proportional to a product of intensity function factors,

evaluated at the observed points, and an exponential whose negative argument is the integral of the intensity function over the observed domain. One difference is the integral over the latent observable, F , in the product factor; this accounts for measurement error. A more subtle but important difference is that the integrand in the exponential is not the same function playing the role of the intensity function in the product factor. There is an average efficiency factor in the exponential, but *not* in the product factor. This is because of a common feature of astronomical surveys noted earlier: the data used for characterization (estimating member latent parameters) are also used for detection. As a result, were one to insert an efficiency factor into the product terms, some of the data would be doubly used. Such considerations appeared explicitly in our derivation; see the text after (A.23). Some heuristic derivations of similar likelihood functions in the astronomical literature have missed this point, instead inserting an $\bar{\eta}(F)$ factor in the detected object integrals in the likelihood function. This corrupts inferences; see Loredo (2004) for further discussion.

This point deserves some elaboration. The statistical literature on sample surveys has of course long been concerned with selection bias. But the typical setting in the sample survey literature is one where an individual is selected by some process, and subsequently fills out a survey (or is otherwise subject to measurement)—*selection is independent of measurement*. Key concepts in sample survey statistics rely on such independence; an example is *inverse probability weighting*, as appears in the well-known Horvitz-Thompson estimator (closely related to the V/V_{\max} method popular in astronomy; Loredo & Wasserman (1995) discuss relationships between such methods and the framework described here). But in astronomical surveys measurement and selection (detection) are typically closely linked and are not independent—selection typically relies on measurement (perhaps done approximately), and object characterization relies on data used for detection. The analysis above treats such cases. In some cases, part of the selection process may be independent of object characterization. For example, in high-energy astrophysics and particle astrophysics settings, there may be an anti-coincidence detector, separate from the main detector, used to exclude events that are likely due to uninteresting backgrounds (but also excluding some interesting events). If the anti-coincidence data are ignored for characterizing detected events, then $\rho(\mathcal{O})$ above should be replaced by $\tilde{\rho}(\mathcal{O}) = F(\mathcal{O})\rho(\mathcal{O})$, where $F(\mathcal{O})$ is a *selection filter function* that accounts for the independent selection process. Other settings with this structure are those where, in some sense, nature is selecting a subsample; that is, we have specified $\rho(\mathcal{O})$ as describing some underlying population, not the actually observable population, which is a subsample due to geometric or other effects beyond the control of the observer. An example in exoplanet demographics arises in modeling transit survey data. Only planetary systems with the right geometry are observable; if $\rho(\mathcal{O})$ describes *all* systems, then a filter function needs to be introduced accounting for geometry-based selection. Of course, transit

data are subject to other selection effects that are tied to the transit measurement process (e.g., only transits with estimated depth greater than a threshold are deemed detections); in these settings, the presence of a filter function does not imply the absence of a detection efficiency, and both types of selection must be accounted for.

Notably, the Poisson process intensity parameter, λ , appears in the likelihood function only in two places: in the factor in front, λ^N , and multiplying the integral in the exponential. As a result, if we adopt a conjugate prior for λ (a gamma distribution), we can easily compute the marginal likelihood function for the ζ parameters. For simplicity, we adopt the limiting case of a uniform prior for λ . Marginalizing over λ and dropping some ζ -independent terms, we find that the marginal likelihood function for ζ takes the form

$$\mathcal{L}_m(\zeta) = \prod_{i=1}^N \int dF \mu(F, r_i; \zeta) \ell_i(F), \quad (\text{A.31})$$

where we have introduced an *effective pseudo-density* for the latent observables, F and r ,

$$\mu(F, r; \zeta) \equiv \frac{h(r)\rho(F, r; \zeta)}{\int dr \int dF \bar{\eta}(F) h(r) \rho(F, r; \zeta)}. \quad (\text{A.32})$$

Equation (A.31) resembles the familiar likelihood function for a binomial point process (i.e., the likelihood function for a fixed-size sample of points independently distributed in some space, found simply by multiplying the point densities), generalized to account for measurement errors described by the member likelihood functions. But the analogy is not exact, because the effective pseudo-density is not a PDF for the *latent member parameters* (F, r) (it does not integrate to unity over (F, r)); rather, it is a probability distribution for the *data* (up to proportionality).

Hierarchical and multilevel models are special cases of *probabilistic graphical models*, and their structures are often described using directed acyclic graphs (DAGs)—nodes, denoting a priori uncertain quantities (random variables), connected by arrows indicating conditional dependence (and, importantly, absent edges indicating conditional independence); shaded nodes indicate quantities that become known (data). Fig. A.5 shows a schematic DAG for the thinned latent marked point process (TLaMPP) framework. Separate plates (boxes containing replicated substructures) depict the conditional independence structure for parts of the joint distribution describing detected and undetected objects (a more detailed DAG would partition the nondetection data among the Δ_j intervals; this would involve nested plates). The numbers of replications for the detection and nondetection plates, N and \bar{N} , are random variables, since the number of objects in the surveyed region is not known a priori, and is informative about the population parameters.

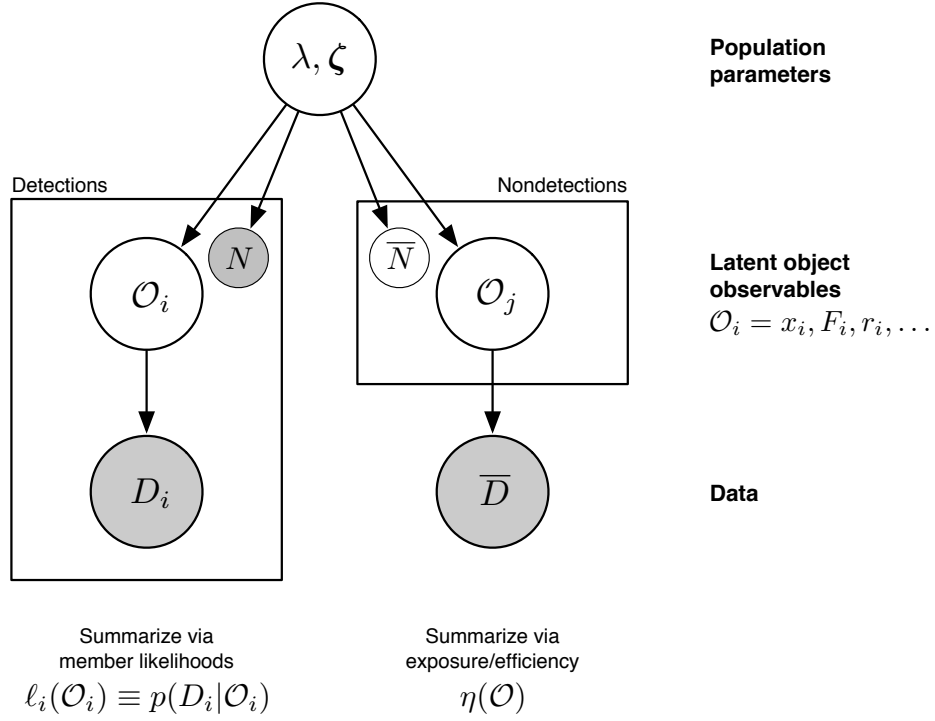


Figure A.5: Schematic DAG for a thinned latent marked point process (TLaMPP) model for luminosity function estimation from survey catalog data. The small N and \bar{N} nodes specify the numbers of replications of the detection and nondetection plates, respectively.

References

- [1] Bayarri, M. J., and Castellanos, M. E. (2007) Bayesian checking of the upper levels of hierarchical models. *Stat. Sci.*, 22, 322–343
- [2] Berger, J. O., Strawderman, W., and Tang, D. (2005) Posterior propriety and admissibility of hyperpriors in normal hierarchical models. *An. Stat.*, 33, 606–646
- [3] Berry, S. M., Carroll, R. J., and Ruppert, D. (2002) Bayesian smoothing and regression splines for measurement error problems. *JASA*, 97(457), 160–169
- [4] Browne, W. J., and Draper, D. (2006) A comparison of Bayesian and likelihood-based methods for fitting multilevel models. *Bayes. An.*, 1, 473–514
- [5] Carlin, B. P., and Louis, T. A. (2000) *Bayes and Empirical Bayes Methods for Data Analysis*. Chapman & Hall/CRC
- [6] Carlin, B. P., Clark, J. S., and Gelfand, A. E. (2006) Elements of hierarchical Bayesian inference. In *Hierarchical modeling for the Environmental Sciences* [ed. J. Clark & A. E. Gelfand], Oxford U. Press, 3–24
- [7] Diaconis, P., and Freedman, D. (1980) Finite exchangeable sequences. *An. Prob.*, 8, 745–764
- [8] Eddington, A. S. (1913) On a formula for correcting statistics for the effects of a known error of observation. *MNRAS*, 73, 359–360
- [9] Eddington, A. S. (1940) The correction of statistics for accidental error. *MNRAS*, 100, 354
- [10] Efstathiou, G., Ellis, R. S., Peterson, B. A. (1988) Analysis of a complete galaxy redshift survey. II — The field-galaxy luminosity function. *MNRAS*, 232, 431–461
- [11] Erdogdu, P., et al. (2006) Reconstructed density and velocity fields from the 2MASS redshift survey. *MNRAS*, 373, 45
- [12] Freudling, W., et al. (1995) Determination of Malmquist bias and selection effects from Monte Carlo simulations. *AJ*, 110, 920
- [13] Gelman, A. (2006) Prior distributions for variance parameters in hierarchical models. *Bayesian An.*, 1, 515–534

- [14] Hendry, M. A. & Simmons, J. F. L. (1994) Optimal galaxy distance estimators. *ApJ*, 435, 515
- [15] Hendry, M. A. & Simmons, J. F. L. (1995) Distance Estimation in Cosmology. *Vistas in Astronomy*. 39, 297
- [16] Hudson, M. J. (1994) Optical galaxies within 8000 km s^{-1} . III. Inhomogeneous Malmquist bias corrections and the Great Attractor. *MNRAS*, 266, 468
- [17] Landy, S. D. & Szalay, A. S. (1992) A general analytical solution to the problem of Malmquist bias due to lognormal distance errors. *ApJL*, 391, 494–501
- [18] Lored, T. J. (2004) Accounting for Source Uncertainties in Analyses of Astronomical Survey Data. In *Maximum Entropy and Bayesian Methods* [ed. Fischer, R., Preuss, R., and Toussaint, U. V.], *American Institute of Physics Conference Series*, 195–206
- [19] Lored, T. J. (2007) in *Statistical Challenges in Modern Astronomy IV*, ASP Conf. Ser. 371, 121
- [20] Lored, T. J. (2013) in *Astrostatistical Challenges for the New Astronomy* [ed. Hilbe, J. M.], Springer, 15–40
- [21] Lored, T. J. and Wasserman, I. M. (1995) Inferring the spatial and energy distribution of gamma-ray burst sources. 1: Methodology. *ApJ Supp*, 96:261–301
- [22] Lored, T. J. and Wasserman, I. M. (1998a) Inferring the Spatial and Energy Distribution of Gamma-Ray Burst Sources. II. Isotropic Models. *AjP*, 502, 75–107
- [23] Lored, T. J. and Wasserman, I. M. (1998b) Inferring the Spatial and Energy Distribution of Gamma-Ray Burst Sources. II. Anisotropic Models. *AjP*, 502, 108–129
- [24] Louis, T. A. (1984) Estimating a population of parameter values using Bayes and empirical Bayes methods. *JASA*, 79:393–398
- [25] Lynden-Bell, D. (1971) A method of allowing for known observational selection in small samples applied to 3CR quasars. *MNRAS*, 155, 95–118
- [26] Lynden-Bell, D., et al. (1988) Spectroscopy and photometry of elliptical galaxies. V — Galaxy streaming towards the new supergalactic center. *ApJ*, 326, 19

- [27] Malmquist, K. G. (1920) A study of the stars of spectral type A. *Medd. Lund Astron. Obs.*, Ser. 2, No. 22, 359–360
- [28] Malmquist, K. G. (1922) On some relations in stellar statistics. *Medd. Lund, Series I.*, 100
- [29] Müller, P., Quintana, F. A. (2004) Nonparametric Bayesian Data Analysis. *Stat. Sci.*, 19, 95–110
- [30] Petit, J.-M., Kavelaars, J. J., Gladman, B. J., and Lored, T. J. (2007) Size distribution of multi-km tnos. In Barucci, A., Boehnhardt, H., Cruikshank, D., and Morbidelli, A., editors, *Kuiper Belt*. University of Arizona Press & Lunar & Planetary Inst. (in press).
- [31] Regier, J., Miller, A., Schlegel, D., Adams, R., McAuliffe, J., Prabhat (2019) Approximate inference for constructing astronomical catalogs from images, *Annals of Appl. Stat.*, 13, 1884–1926
- [32] Schechter, P. L. (1980) Mass-to-light ratios for elliptical galaxies. *AJ*, 85, 801
- [33] Sheth, R. K. (2007) On estimating redshift and luminosity distributions in photometric redshift surveys. *MNRAS*, 378, 709–715
- [34] Sinharay, S., and Stern, H. S. (2003) Posterior predictive model checking in hierarchical models. *J. Stat. Plan. Infer.*, 111, 209–221
- [35] Strauss, M. A. & Willick, J. A. (1995) The density and peculiar velocity fields of nearby galaxies. *Physics Reports*, 261, 271–431
- [36] Szalai-Gindl, J. M., Lored, T. J., Kelly, B. C., Budavári, T., Dobos, L. (2018) GPU-accelerated hierarchical Bayesian estimation of luminosity functions using flux-limited observations with photometric noise, *Astronomy & Computing*, 25, 247–256
- [37] Teerikorpi, P. (1997) Observational Selection Bias Affecting the Determination of the Extragalactic Distance Scale. *Ann. Rev. Astron. Astrophys.*, 35, 101–136
- [38] Wasserman, L. (2005) *All of nonparametric statistics*. Berlin: Springer-Verlag.
- [39] Willick, J. A. (1994) Statistical bias in distance and peculiar velocity estimation. 1: The ‘calibration’ problem. *ApJS*, 92, 1–31
- [40] Willick, J. A. & Strauss, M. A. (1998) Maximum likelihood comparison of Tully-Fisher and redshift data. II. Results from an expanded sample. *ApJ*, 507, 64